Analytical model for a hydrogen atom in a magnetic field: Implications for the diamagnetic shift

Duncan K. Maude ●[*] and Paulina Plochocka

Laboratoire National des Champs Magnétiques Intenses, CNRS-UGA-UPS-INSA, 143 avenue de Rangueil, 31400 Toulouse, France

Zhuo Yang ●[†]

Institute for Solid State Physics, The University of Tokyo, Kashiwa, Chiba, 277-8581, Japan

We propose a simple phenomenological model for a hydrogen atom in a magnetic field which correctly reproduces the results of Makado and McGill's variational calculations for the s, p, d, and f states for orbital quantum numbers $n \leqslant 4$. The expression for the energy of the $1s$ state reveals that it never exhibits true free carrier behavior. Even at high magnetic fields the energy varies as $\alpha_n \hbar \omega_c / 2$, where $\hbar \omega_c = \hbar e B / \mu_r$ is the cyclotron energy and $\alpha_n \simeq 0.84 < 1$. A Taylor expansion of the expression for the energy of the $1s$ state predicts a diamagnetic shift $\Delta E = \sigma B^2$ where $\sigma = \alpha_n^2 e^2 a_B^2 / 4 \mu_r$. This suggests that there is a missing factor of $\alpha_n^2 \simeq 0.71$ in the generally accepted perturbation expression for the diamagnetic shift. This hypothesis is supported by a careful analysis of literature data for shallow donors and excitons in GaAs in the magnetic field.

I. INTRODUCTION

Hydrogen atoms, formed by an electron and a proton which are bound via the Coulomb interaction, occur in vast quantities throughout the universe, both in stars and as gas in interstellar space [1]. In the absence of a magnetic field Schrödinger's equation for the hydrogen atom can be solved, and the allowed energy levels are given by $E_n = -R_y/n^2$, with the Rydberg $R_y = e^2/8\pi\varepsilon a_B$, $a_B = \hbar^2 4\pi\varepsilon/\mu_r e^2$ is the Bohr radius, μ_r is the reduced mass, and $\varepsilon = \varepsilon_r \varepsilon_0$ is the dielectric constant [2,3]. The wave function can be expressed in terms of the radial and angular wave functions as $\Psi(r, \theta, \psi) = R_{nl}(r)Y_{lm}(\theta, \psi)$, where l is the azimuthal quantum number and m is the magnetic quantum number. The hydrogen levels form shells which are labeled s, p, d, and f, often prefixed by the principal quantum number. Typical laboratory-scale magnetic fields have no effect on the hydrogen atom due to the rather large value of the Ryberg $R_y \simeq 13.6\,\text{eV}$.

However, in solid-state physics, analogous hydrogen-like systems exist, for example, shallow donors/acceptors, or photocreated electron-hole pairs know as excitons. In semiconductors, the significantly lower effective masses and the modified dielectric environment, reduce the binding energy by around three orders of magnitude, allowing laboratory-scale magnetic fields to modify the electronic states of hydrogenic shallow impurities and weakly bound excitons [4,5]. The magnetic field can be introduced into the Hamiltonian by replacing the kinetic energy term $\vec{P}^2/2\mu_r$ with the usual Peierls substitution $\vec{P} \rightarrow \hat{P} - e\vec{A}$, where $\vec{A}$ is the magnetic vector potential. Unfortunately, the resulting Hamiltonian is nonintegrable and has no analytical solution [6,7].

Numerical calculations for hydrogen in a magnetic field do exist, and provide reliable results, at least for the lower energy levels. For example, the widely used [8–11] variational calculations of Makado and McGill [12] provide the energy of the hydrogen levels as a function of the dimensionless parameter $\gamma = \hbar\omega_c/2R_y$ for $\gamma = 0 - 10$. While it is possible to directly use the Makado and McGill results to analyze hydrogenic states in a magnetic field, entering the four pages of numerical data is both tedious and time consuming. It would be much more convenient for experimental physicists to have an analytical expression for the evolution of the states in a magnetic field.

In this work, based on our observation that a phenomenological expression, which resembles the Fock-Darwin ground state for an artificial atom [13,14], correctly describes evolution of the $1s$ excitonic state in a magnetic field, we propose an analytical model which is capable of reproducing the magnetic-field evolution of hydrogenic states from the Makado and McGill paper. The parameters in the model have been determined by fitting to the numerical calculations. The model suggests that the generally accepted and widely used perturbation expression for the diamagnetic shift is missing a factor $\alpha_n^2 \simeq 0.71$. We show that this hypothesis is supported by the literature data for shallow donors and excitons in GaAs in a magnetic field [15–20].

The rest of this paper is organized as follows. In Sec. II we present the phenomenological model used to reproduce the Makado and McGill numerical calculations for a hydrogen atom in a magnetic field. We describe the physical influence of each term in the model, the constraints on the six parameters involved for each state, and the fitting procedure used. In Sec. III we use literature data of shallow donors and excitons in magnetic field in GaAs, selected as an almost ideal hydrogenic system, to precisely determine the electron effective mass, static dielectric constant, and reduced exciton mass.

*duncan.maude@lncmi.cnrs.fr
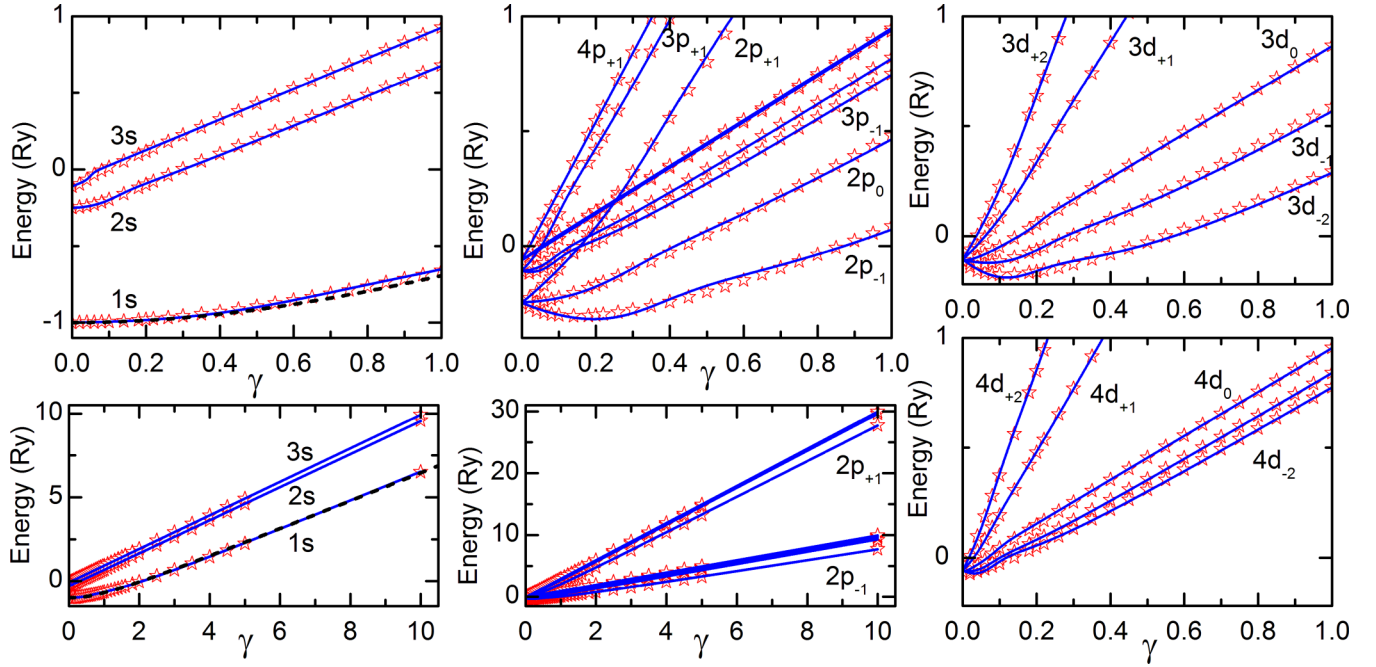†zhuo.yang@issp.u-tokyo.ac.jp

FIG. 1. Symbols show the numerical values of Makado and McGill for the energies of the s, p, and d states versus the dimensionless magnetic field γ in the low field range of interest $\gamma = 0$–1. For the s and p states we also show Makado and McGill results over the full field range $\gamma = 0$–10. The blue lines are calculated using the simple phenomenological model using the parameters in Table I. For the $1s$ state, the black dashed lines are calculated using the simplified expression with no correction term ($\delta = 0$).

From the reduced exciton mass we are able to estimate the hole effective mass, although the problem is ill-posed due to the order of magnitude differences in the electron and hole effective masses. In Sec. IV we compare the diamagnetic shift of the Makado and McGill 1s hydrogen state with the diamagnetic shift of first-order perturbation theory. Finally, in Sec. V we summarize the main conclusions of our work.

II. ANALYTICAL APPROXIMATION TO MAKADO AND MCGILL

The hydrogen states are labeled by their orbital quantum number n, and depending upon the wave function, the z-projection of the angular momentum $L_z = mL$. In the magnetic field n is no longer a good quantum number [21,22], however, for the sake of convenience we continue to use n to the label the states. The magnetic field evolution of the energies of the s, p, and d states ($n \leqslant 4$), taken from the tabulated results of the Makado and McGill variational calculations [12], are shown by the symbols in Fig. 1. The s states display a monotonic increase in energy with field, while the p and d states which have angular momentum, depending upon the magnetic quantum number m, can show a decrease in energy at low fields due to the contribution of the orbital Zeeman energy.

A. Phenomenological model

In the following, we will show that the energy in Rydbergs, of the levels of the hydrogen atom in a magnetic field, are well

described by a simple phenomenological expression:

$$E(\gamma) = -\frac{1}{n^2} - E_0 + \sqrt{E_0^2 + \alpha_n^2 \gamma^2} + \beta_m \gamma + \frac{\delta}{1 + e^{-2\kappa(\gamma - \gamma_0)}}.$$

Following Makado and McGill, the dimensionless magnetic field is defined as $\gamma = \frac{1}{2}\hbar\omega_c/R_y$, which is half of the cyclotron energy in units of the effective Rydberg. For donors or acceptors, the cyclotron energy (and the effective Rydberg) should be calculated using the appropriate band edge electron (m_e^*) or hole effective mass (m_h^*). For excitons, the reduced exciton mass μ_r should be used with $1/\mu_r = 1/m_e^* + 1/m_h^*$. For a given state the model has up to six fitting parameters, namely, three principle parameters $E_0(R_y)$, α_n, and β_m, and three parameters in a correction term $\delta(R_y)$, κ, and γ_0.

The first term in the expression $-1/n^2$ is the zero field energy (in Rydbergs) of the hydrogen states. The third term closely resembles the Fock-Darwin ground state. At high magnetic fields ($\alpha_n^2\gamma^2/E_0^2 \gg 1$) this term is equal to $\alpha_n\gamma$, i.e., a multiple of the cyclotron energy, which with a suitable choice of α_n will reproduce the behavior of free carriers. At low magnetic field ($\alpha_n^2\gamma^2/E_0^2 \ll 1$), the E_0^2 term dominates the square root and the energy evolves according to the first term in the Taylor expansion $[(1 + x^2)^{1/2} \simeq 1 + x^2/2]$, so that $E \propto \alpha_n^2\gamma^2/E_0$, reproducing the expected diamagnetic shift. The second term ($-E_0$) is simply bookkeeping, removing the unwanted $\sqrt{E_0^2}$ contribution of the Fock-Darwin like term at zero magnetic field, ensuring the energy follows the required $E = -1/n^2$ hydrogenic series.

The p, d, and f states have angular momentum, giving rise to the orbital Zeeman term $\beta_m\gamma$. In the Fock-Darwin picture, for the excited states we would have $\beta_m = m$, however, here

TABLE I. Parameters used to reproduce the Makado and McGill numerical solution for hydrogen in a magnetic field.

ψ	n	m	$E_0(R_y)$	α_n	β_m	$\delta(R_y)$	κ	γ_0
$1s^a$	1	0	1	0.84	0	0	–	–
$1s$	1	0	1.38	0.87	0	0.102	3.5	0.6
$2s$	2	0	0.113	0.987	0	0.0455	20	0.12
$3s$	3	0	0	1	0	0.0368	80	0.05
$2p_0$	2	0	0.586	1	0	0.141	6	0.278
$2p_{\pm 1}$	2	± 1	1.139	1.585	$m+0.3$	0.209	6	0.353
$3p_0$	3	0	0.159	1	0	0.0725	20	0.0848
$3p_{\pm 1}$	3	± 1	0.253	1.487	$m+0.5$	0.101	20	0.0855
$4p_0$	4	0	0	1	0	0.0105	30	0.0265
$4p_{\pm 1}$	4	± 1	0	1.5	$m+0.5$	0.00237	20	0.1395
$3d_0$	3	0	0.0505	1	0	0.0243	30	0.2086
$3d_{\pm 1}$	3	± 1	0.497	1.378	$m+0.6$	0.110	10	0.2
$3d_{\pm 2}$	3	± 2	0.762	2.265	$m+0.6$	0.171	10	0.175
$4d_0$	4	0	0.0133	1	0	0.0295	30	0.0887
$4d_{\pm 1}$	4	± 1	0.1746	1.495	$m+0.5$	0.0726	20	0.0697
$4d_{\pm 2}$	4	± 2	0.284	1.987	$m+1.0$	0.114	20	0.0767
$4f_0$	4	0	0.0748	1	0	0.04414	30	0.0568
$4f_{\pm 1}$	4	± 1	0.531	3.47	$m+0.5$	0.216	20	0.0784
$4f_{\pm 2}$	4	± 2	0.813	3.39	$m+1.5$	0.267	20	0.107

[a]Simplified fit with δ forced to zero to allow direct comparison with the diamagnetic shift predicted by perturbation theory.

we treat β_m as a fitting parameter. We also implicitly parameterized the contribution of the cyclotron energy through the coefficient α_n, which is at least partially justified by the fact that n is no longer a good quantum number in magnetic field. Nevertheless, the parameters α_n and β_m are strongly constrained by the following considerations. (i) In the high field limit, the predicted energy evolves linearly with $E \propto (\alpha_n + \beta_m)\gamma$, so that $\alpha_n + \beta_m$ has to be close to the appropriate integer value to reproduce the free-carrier-like behavior. (ii) In a given shell, states with $L_z = |m|L$ are separated from states with $L_z = -|m|L$ by exactly $2|m|\gamma$, so that $\beta_{|m|} - \beta_{-|m|} = 2|m|$. This is imposed by time reversal symmetry, and Makado and McGill give only energies for $m \geqslant 0$ since $E_{-|m|} = E_{|m|} - 2|m|\gamma$ [12].

Neglecting the last term in the expression for the moment (i.e., assuming $\delta = 0$), a reasonable fit of the low field region can be obtained, in particular for the $1s$ ground state. For the s-states there is no orbital Zeeman contribution ($\beta_m = 0$) and the competition between the cyclotron energy and E_0, essentially $\alpha_n^2\gamma^2/E_0^2$, determines the range of γ where a diamagnetic shift is observed. Additionally, α_n is strongly constrained by the slope of the extensive linear region at high fields. The p, d, and f states have an orbital Zeeman contribution, which for $m < 0$ ($\beta_m < 0$) competes with the diamagnetic shift, leading to a negative dispersion at low fields. As before $\alpha_n^2\gamma^2/E_0^2$ determines the width of the diamagnetic field region, while β_m has to chosen to reproduce the negative dispersion. Again, the value of $\alpha_n + \beta_m$ is constrained to be close to the appropriate integer value to correctly reproduce the slope at large magnetic fields.

For all states, reasonable fits to the low field region can be obtained, and the fit can also correctly reproduce the slope in the high field limit. However, the calculated energy lies systematically below the Makado and McGill values at high fields. We therefore have to add a correction δ at high fields. This is the last term in the expression, it is essentially a

smeared out Heaviside step function, with a broadening determined by the parameter κ, and the midpoint (where the correction is $\delta/2$) given by γ_0. This term attempts to correctly reproduce the transition from the regime with bound hydrogen states at low field, to the free carrier region at high field. The parameters κ and γ_0 have to be chosen with some care. If the δ correction is required already at low fields, κ has to be chosen to have a broadening which is sufficiently narrow, so as not to influence the $-1/n^2$ zero field energies. Physically, the correction term takes into account the coupling of the center of mass and orbital motion which controls the transition from a bound state to a free carrier state in the magnetic field.

B. Fitting procedure

To determine the parameters for each of the states, we performed a nonlinear curve fit using a mix of Simplex/Levenberg-Marquardt (SLM) iterations. In a first approach, we impose $\delta = 0$ and fit the low field region to obtain E_0, α_n, and when appropriate, β_m. Values are chosen so that the high field slope is roughly reproduced, albeit with an offset. E_0, α_n, and β_m are then fixed, and we perform SLM iterations to fit with δ, κ, and γ_0 as free parameters (while imposing that the zero field energy does not deviate from the required $-1/n^2$).

The calculated evolution (solid blue lines) is compared with the Makado McGill values (symbols) for the s, p, and d states in Fig. 1. We focus on the low field $\gamma = 0$–1 region where the bound to free carrier transition occurs. For the s and p states, we also show the variation for $\gamma = 0$–10 to highlight the good agreement at high magnetic fields. The model correctly reproduces the low field diamagnetic behavior, negative dispersion for negative values of m, and the linear free carrier behavior at high fields. For the $1s$ state, the black dashed lines are calculated using the simplified expression with no correction term ($\delta = 0$). For $\gamma \geqslant \gamma_0 = 0.6$, the dashed line

lies slightly below the full hydrogen model due to the absence of the correction term with $\delta \simeq 0.1$ (see $1s$ parameters in Table I). To have a feel for the magnetic fields involved, for free excitons in GaAs, $\gamma = 10$ corresponds to a magnetic field $B \simeq 32$ T.

Fitting parameters are given in Table I. When the fitted value of E_0 is equal to an integer value within error, we imposed the integer value, e.g., $E_0 = 0, 1$. Similarly, α_n has been forced to integer values when appropriate. For states with angular momentum, β_m was manually adjusted to fit the negative dispersion, while α_n was evaluated using SLM iterations to fit the high field region where the slope is given by $(\alpha_n + \beta_m)\gamma$. For the $1s$ state, we give two parameter sets. The first is a simplified version, where we forced $\delta = 0$. The absence of the correction term produces a slightly worse fit (dashed lines in Fig. 1) using a marginally different value of α_n.

The agreement between the Makado and McGill numerical results and our simple model, which agree to better than a few percent in Fig. 1, is more than good enough over the full range of γ values to make the model useful for solid-state physicists. However, the model cannot be expected to reproduce the four to five digit accuracy of the Makado and McGill calculations.

C. $1s$ state

The evolution of the $1s$ ground state in a magnetic field is important for exciton physics investigated using magnetooptical techniques. It is also required, together with the evolution of the excited p states, to interpret the observed transitions in shallow donor magnetospectroscopy. It should be emphasized that the $1s$ state is unique, in that it never exhibits truly free carrier behavior, even at the highest magnetic fields. The fitted value of $\alpha_n \simeq 0.84$–0.87 depending on the model, is $\simeq 13$–16% below the free carrier $\alpha_n = 1$ value. The large value of $E_0 \simeq 1$ gives rise to a relatively wide region at low magnetics fields for which a diamagnetic shift ($\Delta E \propto \gamma^2$) is observed. In contrast, the excited s-states have little ($2s$) or no ($3s$) diamagnetic contribution ($E_0 = 0$ for $3s$).

III. GaAs AS A MODEL SYSTEM

Hydrogenic shallow donor states in GaAs are a relatively simple system as the only parameters involved are the electron effective mass and the relative dielectric constant. After determining precise values for these parameters we turn our attention to excitons in GaAs, a significantly more complex problem with the uncertain value of the hole effective mass due to the heavy-hole/light-hole mixing in the valence band [23–25]. The objective here is to provide a reliable parameter set required to compare the measured and predicted diamagnetic shift in Sec. IV.

A. Shallow donors

GaAs is a direct gap semiconductor with a small electron effective mass and isotropic conduction and valence bands [23]. The effective Rydberg for a shallow donor is small, $R_y \simeq 5.8$ meV [26], making GaAs an ideal system to investigate hydrogenic shallow donor states. Photoconductivity measurements on high purity GaAs samples were performed
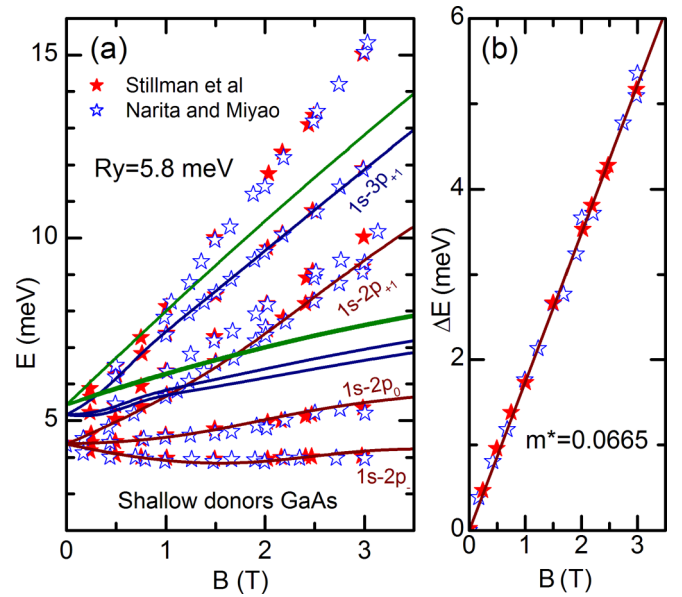

FIG. 2. (a) Symbols are the measured shallow donor transition energies in high purity GaAs versus magnetic field from the photoconductivity measurements of Stillman *et al.* [15] and Narita and Miyao [16]. The curves are the calculated transition energies using the phenomenological model for the hydrogen atom as described in the text. They are labeled where possible. The color indicates the $1s \rightarrow 2p_{0,\pm1}$ (wine), $1s \rightarrow 3p_{0,\pm1}$ (navy), and $1s \rightarrow 3p_{0,\pm1}$ (olive) transitions. (b) Symbols show the measured splitting of the $1s \rightarrow 2p_{\pm1}$ transitions versus magnetic field. The solid line is a linear least squares fit used to determine the effective mass $m_e^* = (0.0665 \pm 0.0005)m_e$.

over 50 years ago to investigate the $1s \rightarrow 2p$ and $1s \rightarrow 3p$ transitions in magnetic fields up to 3 T. In Fig. 2(a) we plot the digitized data from the publications of Stillman *et al.* [15] and of Narita and Miyao [16]. Despite the measurements being performed on presumably different samples (the donor involved is not specified in either paper, most likely it is Si), there is a remarkable overlap between the two data sets. The solid lines are the predicted transition energies calculated using the phenomenological model for hydrogen in a magnetic field. The excellent agreement between theory and experiment confirms the hydrogen-like nature of shallow donors in GaAs.

To determine the effective mass we use the fact that the separation of the $2p_{\pm1}$ states is exactly $\hbar\omega_c$. In the inset of Fig. 2(b) we plot the splitting of the $1s \rightarrow 2p_{\pm1}$ transitions versus magnetic field. As expected, the splitting varies linearly with magnetic field, and a linear fit gives a slope of 1.73922 ± 0.0087 meV/T. The effective mass is therefore $m_e^* = (0.0665 \pm 0.0005)m_e$ (as previously determined by Stillman *et al.* [15]). The only unknown parameter in the hydrogen model is then the relative dielectric constant. Fitting to the transitions, almost perfect agreement is obtained using $m_e^* = 0.0665m_e$ and $\varepsilon_r = 12.5 \pm 0.1$. The value of the dielectric constant agrees within error with the measured value of the static (low frequency) dielectric constant $\varepsilon_r \simeq 12.4$ in GaAs at low temperatures, but is significantly larger the the high frequency value of $\varepsilon_\infty = 10.58$ [27,28]. Using $\varepsilon_r = 12.5$ the calculated shallow donor binding energy is then
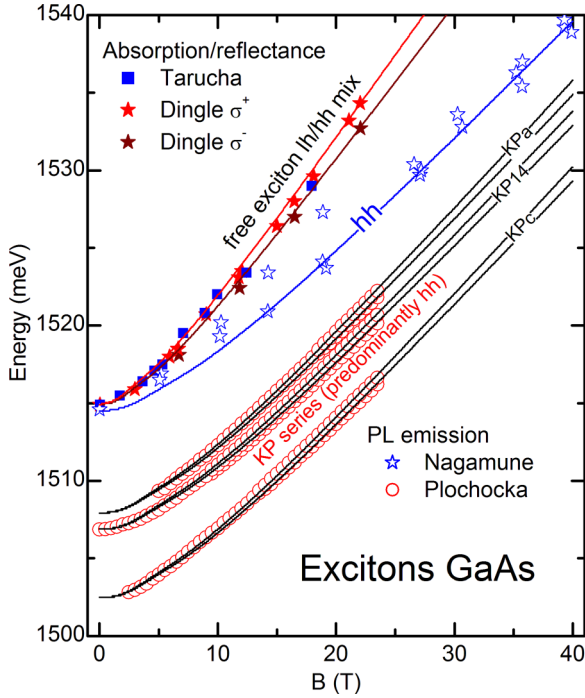
FIG. 3. Low-temperature ($T \leqslant 4$ K) exciton absorption/ emission in GaAs. Closed symbols are absorption/refelectance measurements which have a predominantly free exciton light hole character due to the light hole-heavy hole mixing. Open symbols are PL emission of weakly bound excitons which have a predominantly heavy hole character. Data is taken from Refs. [17–20]. The curves are calculated from the evolution of the 1s excitonic state obtained from the full model of the hydrogen atom.

$R_y = 5.8 \pm 0.1$ meV. The states which are not reproduced by the model in Fig. 2 were identified by the authors of Refs. [15,16] as magnetic field states which do not originate from the bound states of the hydrogenic donor [21,22].

B. Excitons

Having determined reliable values for the electron effective mass and the relative dielectric constant, we are now in a position to analyze the more delicate case of excitons in a magnetic field. In Fig. 3, we plot the energy of the 1s excitonic state in bulk GaAs versus magnetic field measured using absorption, reflectance, and photoluminescence (PL) emission at low temperatures ($T \leqslant 4$ K). The most precise data are provided by the polarization resolved reflectance measurement of Dingle [17] obtained in static (DC) magnetic fields up to 22 T. Nevertheless, the absorption data of Tarucha et al. [18] obtained in pulsed magnetic fields agree within error with the reflectivity results.

In contrast, the PL emission data of Nagamune et al. [19] also obtained in pulsed magnetic fields, lie well below the absorption/reflectance data at high magnetic fields suggesting a significantly heavier reduced exciton mass. At intermediate magnetic fields, two features are observed in the PL, with the higher-energy feature close to the absorption/reflectance data. This suggests that the lower-energy feature which dominates

TABLE II. Reduced mass (μ_r) and approximate effective Landé g-factors extracted by fitting the full version of the 1s hydrogen model to the exciton emission/absorption data for GaAs in Fig. 3. Other parameters are calculated from the reduced mass, using the electron mass $m_e^* = 0.0665 m_e$ and relative dielectric constant $\varepsilon_r = 12.5$ from the shallow donor fit. The diamagnetic coefficient σ is estimated from a Taylor expansion of the simplified expression for the 1s state. No attempt has been made to obtain accurate values for the exciton g-factors used.

Exciton	$\mu_r(m_e)$	$m_h^*(m_e)$	R_y(meV)	$\sigma(\mu eV/T^2)$	g
Dingle	0.048 ± 0.001	0.17 ± 0.02	4.2	124	1.2
Naga	0.064 ± 0.003	1.7 ± 1.1	5.6	51	–
KPa	0.060 ± 0.001	0.66 ± 0.1	5.3	61	0.4
KP14	0.062 ± 0.001	0.88 ± 0.2	5.4	57	0.4
KPc	0.060 ± 0.001	0.66 ± 0.1	5.3	61	0.4

the PL at high magnetic fields in the Nagamune data, is not the free exciton transition. A natural explanation for the three data sets would be the following. (i) Reflectance/absorption measures the free exciton transition with a considerably reduced hole mass due to the heavy-hole/light-hole mixing. (ii) In PL, before recombining, photocreated excitons move to a defect or impurity site to form weakly bound excitons. The weak confining potential is nevertheless sufficient to lift the heavy-hole/light-hole degeneracy, reducing the mixing, giving the exciton an essentially heavy-hole character.

In Fig. 3 we also plot polarization resolved PL emission from the so-called KP series of lines, first reported by Kunzel and Ploog [29] and observed in high quality MBE grown GaAs using As$_4$ as a source. They are tentatively thought to arise from the radiative recombination of excitons weakly bound to donor pairs with different separations [30,31]. The three strong KP lines shown here were measured by Plochocka et al. [20] at pumped helium temperatures, using microphotoluminescence on a single GaAs nano wire, with sufficiently large dimensions that it has the properties of bulk GaAs.

The solid lines in Fig. 3 are the fitted evolution of the excitonic emission/absorption using the full hydrogen model for the 1s states. The obtained fitting parameters are given in Table II. For the polarization resolved data, the transitions were fitted assuming a Zeeman splitting of $g\mu_B B$ where g is the effective exciton g-factor. The only fitting parameter is then the reduced mass μ_r and the other parameters were calculated using the electron effective mass, and relative dielectric constant obtained from the shallow donor spectroscopy. The problem of calculating the hole effective mass is ill-posed when the reduced mass approaches the electron effective mass. A small error in the reduced mass creates a large error in the hole's effective mass. Nevertheless, the free exciton state observed in absorption/reflectance has a mass which is much less than the accepted heavy hole mass $m_{hh}^* \simeq 0.62$, while still being considerably heavier than the accepted light hole mass $m_{lh}^* \simeq 0.087$ in GaAs [23–25]. This suggests that for the free exciton, in the absence of a confinement potential which lifts the heavy hole/light hole degeneracy, there is a strong mixing of the two states. The exciton states observed in emission
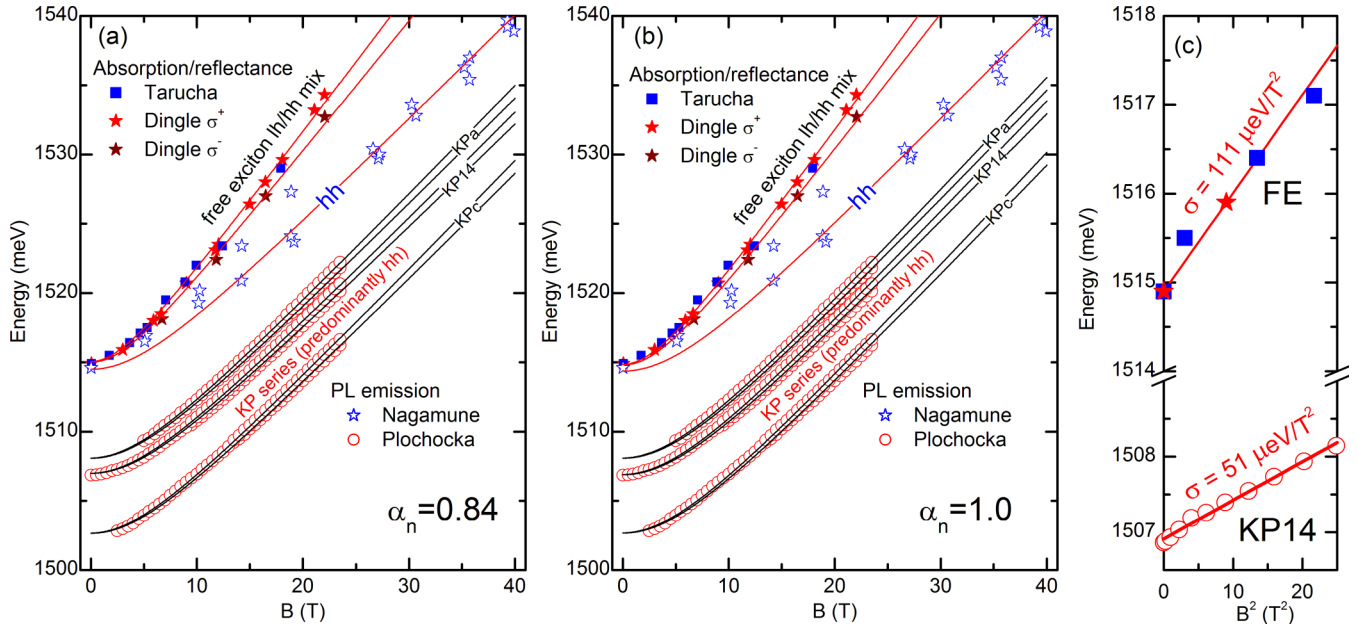
FIG. 4. (a), (b) Low-temperature ($T \leqslant 4$ K) exciton absorption/emission in GaAs from references [17–20]. The curves are calculated from the evolution of the $1s$ excitonic state obtained from the simplified ($\delta = 0$) model of the hydrogen atom with $\alpha_n = 0.84$ (Makado and McGill diamagnetic shift) and $\alpha_n = 1$ (perturbation approach diamagnetic shift). (c) Energy of the free exciton reflectance/absorption and KP14 exciton emission versus B^2 for $B \leqslant 5$ T. The symbols are the same as in panels (a), (b). The solid red lines are least-squares linear fits used to extract the diamagnetic shift.

have hole masses which agree within error with the accepted literature value for the heavy hole mass in GaAs.

IV. DIAMAGNETIC SHIFT

At low magnetic fields, a first-order perturbation-type approach gives the diamagnetic shift of the $1s$ ground state as [4,5]

$$\Delta E = \frac{4\pi^2 \varepsilon^2 \hbar^4}{e^2 \mu_r^3} B^2 = \frac{e^2 a_B^2}{4\mu_r} B^2.$$

This result is widely used to extract the effective mass/Bohr radius from the experimental diamagnetic shift [32–35]. The diamagnetic shift arises from the magnetic-field-induced compression of the exciton wave function due to the additional parabolic confinement potential. Tightly bound excitons or impurity states with highly localized wave functions will have very small diamagnetic shifts ($\simeq 1\,\mu\text{eV/T}^2$). In contrast, weakly bound states, for example, shallow donors, or excitons in GaAs, have a large Bohr radius $a_B \simeq 10$ nm and a relatively large diamagnetic shift $\simeq 100\,\mu\text{eV/T}^2$.

Using the simplified phenomenological expression ($\delta = 0$) the predicted evolution of the hydrogenic excitonic $1s$ state in magnetic field can be written as

$$E = -2R_y + R_y \sqrt{1 + \frac{\alpha_n^2}{R_y^2}\left(\frac{\hbar e B}{2\mu_r}\right)^2},$$

where $\alpha_n = 0.84$, and $R_y = e^2/8\pi\varepsilon a_B$ is the exciton binding energy or effective Rydberg. Using a Taylor expansion we can write the diamagnetic shift

$$\Delta E = \frac{\alpha_n^2}{2R_y}\left(\frac{\hbar e B}{2\mu_r}\right)^2 = \alpha_n^2 \frac{e^2 a_B^2}{4\mu_r} B^2,$$

which differs from the usual diamagnetic shift by a factor $\alpha_n^2 \simeq 0.71$. Thus, the analytical approximation to the Makado and McGill variational calculation for the $1s$ hydrogenic state in a magnetic field suggests that the widely used first-order perturbation expression for the diamagnetic shift is missing a factor $\alpha_n^2 \simeq 0.71$. This will have a significant effect on the reduced mass/Bohr radius extracted from experiment.

A. Simplified $1s$ hydrogen model fit

To test this hypothesis, we fitted the GaAs exciton data using the simplified hydrogen model ($\delta = 0$), using $\alpha_n = 0.84$, and $\alpha_n = 1$, corresponding to the Makado and McGill, and perturbation approach diamagnetic shifts, respectively. The results of such a fit can be seen in Figs. 4(a) and 4(b). In both cases the fits are in good agreement with the data over the full field range, although the parameters extracted from the fits (summarized in Table III) are significantly different.

The fit with $\alpha_n = 0.84$ produces reduced exciton masses which are quite similar to those extracted from the full hydrogen model, although the calculated heavy hole masses no longer agree within error with the accepted literature values [23–25]. This is in a large part due to the ill-posed nature of the hole mass calculation when the reduced effective mass is close to the electron effective mass.

In contrast, for the $\alpha_n = 1$ fit, the reduced exciton masses are significantly overestimated. For the heavy hole-like excitons observed in emission, it even makes no sense to calculate the mass since the reduced mass is higher than the electron

TABLE III. Reduced exciton mass (μ_r) extracted by fitting the simplified ($\delta = 0$) version of the 1s hydrogen model to the exciton emission/absorption data for GaAs in Fig. 4. We fitted using $\alpha_n = 0.84$ (Makado and McGill diamagnetic shift) and $\alpha_n = 1$ (perturbation theory diamagnetic shift). Other quantities are calculated using $m_e^* = 0.0665 m_e$ and $\varepsilon_r = 12.5$ from the shallow donor fit. The diamagnetic coefficient σ is calculated from the measured reduced mass using a Taylor expansion of the simplified expression for the 1s state. The exciton g-factors used are the same as in Table II. The abbreviation ns signifies that there is "no sense" to calculate an unphysical negative value for the mass.

Exc	α_n	$\mu_r(m_e)$	$m_h^*(m_e)$	R_y(meV)	σ(μeV/T^2)
Dingle	0.84	0.049 ± 0.001	0.19 ± 0.02	4.3	115
Naga	0.84	0.064 ± 0.003	1.7 ± 1.1	5.5	52
KPa	0.84	0.062 ± 0.001	0.9 ± 0.2	5.4	57
KP14	0.84	0.063 ± 0.001	1.2 ± 0.3	5.5	54
KPc	0.84	0.062 ± 0.001	0.9 ± 0.2	5.4	57
Dingle	1.0	0.056 ± 0.001	0.35 ± 0.02	4.9	109
Naga	1.0	0.073 ± 0.003	ns	6.4	49
KPa	1.0	0.071 ± 0.001	ns	6.2	54
KP14	1.0	0.072 ± 0.001	ns	6.3	51
KPc	1.0	0.071 ± 0.001	ns	6.2	54

effective mass, leading to unphysical negative values for the hole mass. The values of the expected diamagnetic coefficients, calculated from the Taylor expansion, are very similar for the two cases, indicating that similar diamagnetic coefficients will produce very different reduced masses depending upon the value of α_n used.

B. Direct analysis of the diamagnetic shift

Finally, we investigate the outcome of directly analyzing the slope of the low field diamagnetic shift. In Fig. 4(c) we plot the energy of the free exciton reflectance/absorption and KP14 exciton emission versus B^2 for magnetic fields less than 5 T. In both cases the energy of the emission shifts linearly showing a clear diamagnetic shift $\Delta E \propto B^2$. We are unable to analyze other exciton lines due to the lack of data at low magnetic fields. The solid lines are least squares linear fits to the data.

For the free exciton, fitting to the Dingle reflectance data we obtain a diamagnetic shift of $\sigma = 111 \pm 10\,\mu$eV/T^2. Here the error was estimated from a global fit to the Dingle and Tarucha (lower quality absorption data in pulsed fields) data sets which produces a diamagnetic coefficient which is approximately 10% lower. This gives a reduced mass $\mu_r = (0.0496 \pm 0.002)m_e$, and a hole mass of $m_h = (0.195 \pm 0.02)m_e$ for $\alpha_n = 0.84$, in agreement with the mass deduced using the hydrogen model. In contrast, assuming $\alpha_n = 1$ (perturbation theory diamagnetic shift) gives a reduced mass $\mu_r = (0.0557 \pm 0.002)m_e$, and a hole mass of $m_h = (0.344 \pm 0.08)m_e$ which is twice the expected value (see, e.g., Table II or Table III).

The extracted diamagnetic shift for the KP14 emission $\sigma = 51 \pm 2\,\mu$eV/T^2 gives reduced masses of $\mu_r = (0.064 \pm 0.001)m_e$ ($\alpha_n = 0.84$) and $\mu_r = (0.072 \pm 0.001)m_e$ ($\alpha_n = 1$). The latter reduced mass is unphysical since it requires the hole mass to be negative. For $\alpha_n = 0.84$, the hole mass $m_h^* = 1.9 \pm 0.7$ has a large error due to the ill posed nature of the problem, while nevertheless remaining physical. Thus, a direct analysis of the diamagnetic shift at low magnetic fields supports the conclusion that a factor of $\alpha_n^2 \simeq 0.71$ is missing from the standard perturbation expression for the diamagnetic coefficient.

V. CONCLUSION

We developed an analytical model for the hydrogen atom in a magnetic field based on our experimental observation that a phenomenological expression resembling the Fock-Darwin ground state describes well the evolution of the 1s hydrogenic ground state. Our model correctly reproduces the results of the variational calculations of Makado and McGill [12] for the s, p, d, and f states for orbital quantum numbers $n \leqslant 4$. We used the model to analyze shallow donor transitions and exciton absorption/emission in GaAs in magnetic field. The model, when used to analyze the shallow donor transitions, provides rather precise measurements of the electron effective mass $m_e^* = (0.0665 \pm 0.00050)m_e$, and the low frequency relative dielectric constant $\varepsilon_r = 12.5 \pm 0.1$. The exciton physics is a much more complex proposition due to heavy-hole/light-hole mixing, and the ill-posed nature of the problem due to the order of magnitude difference in the electron and heavy hole effective masses. Nevertheless, the hole masses found agree within error with the literature data.

A Taylor expansion of the simplified analytical expression for the 1s ground state reveals that the expected diamagnetic shift differs from the predictions of perturbation theory by a factor of $\alpha_n^2 \simeq 0.71$. This arises since the 1s state never exhibits true free carrier behavior. Even at the highest magnetic fields the energy shifts as $\alpha_n \hbar \omega_c / 2$ with $\alpha_n \simeq 0.84 < 1$. This suggests that a factor of $\alpha_n^2 \simeq 0.71$ is missing from the standard expression for the diamagnetic shift which should read $\Delta E = \sigma B^2$ where $\sigma = \alpha_n^2 e^2 a_B^2 / 4\mu_r$. Our analysis of the exciton magnetoabsorption/emission in GaAs supports this hypothesis. The values of the exciton reduced mass obtained assuming $\alpha_n^2 = 1$ lead to hole masses which are too large or even unphysical (negative). In contrast, using $\alpha_n^2 \simeq 0.71$ gives reasonable hole masses which mostly agrees within error with the full hydrogen model.

This finding suggests that effective masses, determined from the low field $\Delta E = \sigma B^2$ throughout the literature, need to be corrected to take into account the missing numerical factor $\alpha_n^2 \simeq 0.71$ in the generally accepted expression for the diamagnetic shift.

ACKNOWLEDGMENTS

[1] W. Grochala, First there was hydrogen, Nat. Chem. **7**, 264 (2015).

[2] A. I. M. Rae and J. Napolitano, *Quantum Mechanics*, 6th ed. (CRC Press, Boca Raton, FL, 2015).

[3] C. Cohen-Tannoudji, B. Diu, and F. Laloë, *Quantum Mechanics Volume1* (Wiley, Berlin, 2019).

[4] N. Miura, *Physics of Semiconductors in High Magnetic Field* (Oxford University Press, New York, 2007).

[5] K. Cong, G. T. Noe II, and J. Kono, Excitons in Magnetic Fields, in *Encyclopedia of Modern Optics*, 2nd ed., edited by B. D. Guenther and D. G. Steel (Elsevier, Oxford, 2018), pp. 63–81.

[6] H. Friedrich and H. Wintgen, The hydrogen atom in a uniform magnetic field - An example of chaos, Phys. Rep. **183**, 37 (1989).

[7] M. Aßmann, J. Thewes, D. Fröhlich, and M. Bayer, Quantum chaos and breaking of all anti-unitary symmetries in Rydberg excitons, Nat. Mater. **15**, 741 (2016).

[8] A. Miyata, P. Mitioglu, A Plochocka, O. Portugall, J. T. W. Wang, S. D. Stranks, H. J. Snaith, and R. J. Nicholas, Direct measurement of the exciton binding energy and effective masses for charge carriers in organic-inorganic tri-halide perovskites, Nat. Phys. **11**, 582 (2015).

[9] K. Galkowski, A. Mitioglu, A. Miyata, P. Plochocka, O. Portugall, G. E. Eperon, J. T.-W. Wang, T. Stergiopoulos, S. D. Stranks, H. J. Snaith, and R. J. Nicholas, Determination of the exciton binding energy and effective masses for methylammonium and formamidinium lead tri-halide perovskite semiconductors, Energy Environ. Sci. **9**, 962 (2016).

[10] Z. Yang, A. Surrente, K. Galkowski, N. Bruyant, D. K. Maude, A. A. Haghighirad, H. J. Snaith, P. Plochocka, and R. J. Nicholas, Unraveling the exciton binding energy and the dielectric constant in single-crystal methylammonium lead triiodide perovskite, J. Phys. Chem. Lett. **8**, 1851 (2017).

[11] Z. Yang, A. Surrente, K. Galkowski, A. Miyata, O. Portugall, R. J. Sutton, A. A. Haghighirad, H. J. Snaith, D. K. Maude, P. Plochocka, and R. J. Nicholas, Impact of the halide cage on the electronic properties of fully inorganic cesium lead halide perovskites, ACS Energy Lett. **2**, 1621 (2017).

[12] P. C. Makado and N. C. McGill, Energy levels of a neutral hydrogen-like system in a constant magnetic field of arbitrary strength, J. Phys. C **19**, 873 (1986).

[13] V. Fock, Bemerkung zur Quantelung des harmonischen Oszillators im Magnetfeld, Z. Phys. **47**, 446 (1928).

[14] C. G. Darwin, The diamagnetism of the free electron, Math. Proc. Cambridge Philos. Soc. **27**, 86 (1931).

[15] G. E. Stillman, C. M. Wolfe, and J. O. Dimmock, Magnetospectroscopy of shallow donors in GaAs, Solid State Commun. **7**, 921 (1969).

[16] S. Narita and M. Miyao, Shallow donor states in high purity GaAs in magnetic field, Solid State Commun. **9**, 2161 (1971).

[17] R. Dingle, Magneto-optical investigation of the free-exciton reflectance from high-purity epitaxial GaAs, Phys. Rev. B **8**, 4627 (1973).

[18] S. Tarucha, H. Okamoto, Y. Iwasa, and N. Miura, Exciton binding energy in GaAs quantum wells deduced from magneto-optical absorption measurement, Solid State Commun. **52**, 815 (1984).

[19] Y. Nagamune, Y. Arakawa, S. Tsukamoto, M. Nishioka, S. Sasaki, and N. Miura, Photoluminescence spectra and anisotropic energy shift of GaAs quantum wires in high magnetic fields, Phys. Rev. Lett. **69**, 2963 (1992).

[20] P. Plochocka, A. A. Mitioglu, D. K. Maude, G. L. J. A. Rikken, A. Granados del Águila, P. C. M. Christianen, P. Kacman, and H. Shtrikman, High magnetic field reveals the nature of excitons in a single GaAs/AlAs core/shell nanowire, Nano Lett. **13**, 2442 (2013).

[21] M. Shinada, O. Akimoto, H. Hasegawa, and K. Tanaka, On the nodal surfaces of hydrogen eigenfunctions in a magnetic field, J. Phys. Soc. Jpn. **28**, 975 (1970).

[22] N. Kuroda, Y. Nishina, H. Hori, and M. Date, Validity of the conservation rule of nodal surface numbers in the wave function of hydrogenic exciton in magnetic field, Phys. Rev. Lett. **48**, 1215 (1982).

[23] S. Adachi, GaAs, AlAs, and $Al_xGa_{1-x}As$: Material parameters for use in research and device applications, J. Appl. Phys. **58**, R1 (1985).

[24] A. L. Mears and R. A. Stradling, Cyclotron resonance and Hall measurements on the hole carriers in GaAs, J. Phys. C **4**, L22 (1971).

[25] P. Lawaetz, Valence-band parameters in cubic semiconductors, Phys. Rev. B **4**, 3460 (1971).

[26] J. Wagner and M. Ramsteiner, Binding energies of shallow donors in semi-insulating GaAs, J. Appl. Phys. **62**, 2148 (1987).

[27] I. Strzalkowski, S. Joshi, and C. R. Crowell, Dielectric constant and its temperature dependence for GaAs, CdTe, and ZnSe, Appl. Phys. Lett. **28**, 350 (1976).

[28] W. J. Moore and R. T. Holm, Infrared dielectric constant of gallium arsenide, J. Appl. Phys. **80**, 6939 (1996).

[29] H. Künzel and K. Ploog, The effect of As_2 and As_4 molecular beam species on photoluminescence of molecular beam epitaxially grown GaAs, Appl. Phys. Lett. **37**, 416 (1980).

[30] M. S. Skolnick, C. W. Tu, and T. D. Harris, High-resolution spectroscopy of defect-bound excitons and acceptors in GaAs grown by molecular-beam epitaxy, Phys. Rev. B **33**, 8468 (1986).

[31] M. S. Skolnick, D. P. Halliday, and C. W. Tu, Zeeman spectroscopy of the defect-induced bound-exciton lines in GaAs grown by molecular-beam epitaxy, Phys. Rev. B **38**, 4165 (1988).

[32] G. Saintonge and J. L. Brebner, Magneto-optical properties of the $Ga_xIn_{1-x}Se$ system near the fundamental band gap, Phys. Rev. B **30**, 1957 (1984).

[33] N. Miura, Solid state physics in megagauss fields generated by electromagnetic flux compression and single-turn coils, Phys. B: Condens. Matter **201**, 40 (1994).

[34] M. Hirasawa, T. Ishihara, T. Goto, K. Uchida, and N. Miura, Magnetoabsorption of the lowest exciton in perovskite-type compound $(CH_3NH_3)PbI_3$, Phys. B: Condens. Matter **201**, 427 (1994).

[35] A. V. Stier, K. M. McCreary, B. T. Jonker, J. Kono, and S. A. Crooker, Exciton diamagnetic shifts and valley Zeeman effects in monolayer WS_2 and MoS_2 to 65 Tesla, Nat. Commun. **7**, 10643 (2016).